Analysis of the Planar Electrode Morphology for Capacitive Chemical Sensors

L. E. B. Ribeiro and F. Fruett
School of Electrical and Computer Engineering - FEEC
State University of Campinas – UNICAMP
Campinas, Brazil
e-mail: luizebr@dsif.fee.unicamp.br and fabiano@dsif.fee.unicamp.br

***Abstract* — Three different electrode structures are compared in this work: conventional interdigitated electrodes (IDE), serpentine electrodes (SRE) and ring-shaped electrodes (RSE). Simulation results and experimental characterization of these electrodes showed that ring-shaped electrodes have a slight capacitance increase per unit of area, thus being more sensitive when used as a capacitive sensor. Furthermore, the ring-shaped electrodes are more suitable in process that requires dripping, for better use of the drop distribution. This is the case of liquid substances or sensors with sensitive elements such as zeolite.**

Keywords - interdigitated electrodes; ring-shaped electrodes; serpentine electrodes; capacitive sensors; electrode structure; interdigital electrodes.

I. INTRODUCTION

IDE as capacitive microstructures have been widely used in electronics applications such as surface acoustic wave devices [1], thin-film acoustic electronic transducers [2], tunable devices [3], dielectric spectroscopy [4], dielectric studies on thin films [5][6], humidity and chemical sensors [7][8], etc. They possess interesting features, such as signal strength control by changing its dimensions, multiple physical effects in the same structure, simplified modeling in two dimensions when the aspect ratio of the electrode length to the space wavelength IDE is large, and can be used in a wide range of frequencies [7]. Moreover, it can be manufactured using inert substrates with multiple materials with different fabrication processes, or even microfluidic compatible. Capacitive microstructures used as chemical sensor, typically have one sensitive layer deposited over the electrodes. Polymers have been used for organic vapor sensing because they exhibit rapid reversible vapor sorption and are easy to apply as thin or thick films by a variety of techniques [9]. The polymer layer can be chosen according to its affinity to a particular molecule or set of molecules one wishes to detect. If several sensors with different polymer layers are used to make a sensor array it is then possible to evaluate complex organic vapor samples. These sensor arrays can be part of a so-called electronic nose. Another possibility is the use of flexible substrates such as sensing element. As an example the use of polyimide [10] and plastic foil [11].

Interdigitated electrodes analytical characterization have been received many efforts in order to improve their capacitance by exploring their geometrical parameters. Igreja et al developed a theoretical model of capacitance for this structure [12]. These capacitors have also been simulated using different tools. They have typically been adopted as a sensor because of the low-power consumption of capacitive transduction mechanism and being compact with a large contact area and relative ease of manufacture. Some authors have analyzed other morphologies such as serpentine, spiral and concentric rings electrodes, in order to improve design performance. Moreover, aside from the different morfologies, several strategies have been employed to increase and improve its ability as a sensor, for example the deposition of a more sensitive layer on the electrodes. The sensor can also have its selectivity improved by the deposition of compounds such as zeolite for detection of air humidity or gases [13].

In this work, we study different geometries of electrodes instead of the materials used to maximize capacitance per area. We can thus improve the sensitivity of capacitive sensors by increasing the total capacitance of capacitive microstructures. Here, we compare the conventional IDE, the serpentine electrodes (SRE) and ring-shaped electrodes (RSE). These electrodes are compared in detail as generic capacitive transducers by numerical simulations. In these simulations, the geometric parameters that most influence on the total capacitance are shown. We measure the capacitance of these thin-film electrodes made of titanium and gold on a glass substrate. Finally, we compare the experimental results with the theoretical analysis, including simulations.

In Section II, the different electrodes designs and their geometrical parameters are shown. They are the main data to the numerical simulation, which is explained in the Section III. The fabrication process is described in section IV. Subsequently, the values of electrical and geometrical characterization are shown in section V. The results are compared and discussed in section VI. Finally, the conclusion is presented in section VII.

II. METHODS AND MATERIALS

The layouts of some interdigitated electrode pairs are shown in Figure 1. Although they were designed with the same area, each structure has a particular capacitance. Therefore, they have different sensitivities as capacitive transducer only because of their different geometric structure.

 ISBN: 978-1-61208-426-8

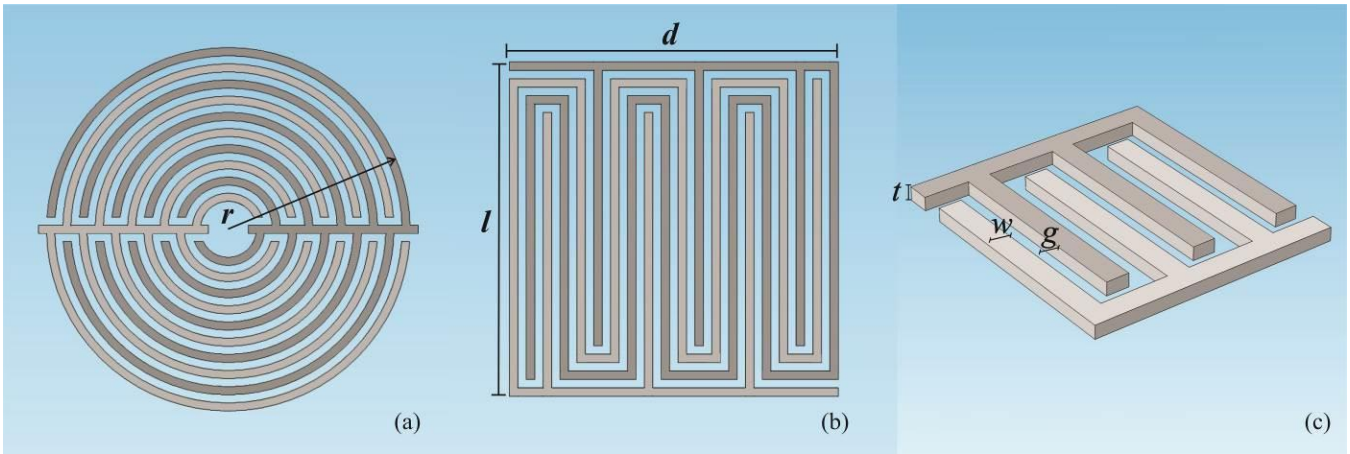

Figure 1. Ring-shape electrode (a), serpentine electrode (b) and interdigitated electrode (c) structures and used parameters.

We simulate the capacitive structures of IDE, SRE and RSE with the same area, same substrate and the same top layer, calculating and comparing the capacitance of each structure using the multiphysics numerical simulator: COMSOL Multiphysics (Comsol Inc., Stockholm, Sweden). This software, based on partial differential equations with the finite element method has been used in the literature to calculate distribution of potential field in similar structures. Figure 2 depicts the simulated structure showing the 3D multislice view of the electrical potential distribution around RSE with 20 fingers.

Multiple simulations were performed to compare dimensions that are relevant to increase the difference between the capacitances. The main geometrical parameters analyzed are the electrode length, the gap between the electrodes, the electrode width (always kept as same value as gap), the thickness of electrodes and the number of fingers. The electrical properties of the substrate and the top layer are also included in the simulator. Because of the differences between the vertical and horizontal dimensions (millimeters to micrometers) critical to reduce the time simulation, we have applied the extrapolation method, presented in the Rivadeneyra work [14]. The thickness has been set to 20% of electrode width.

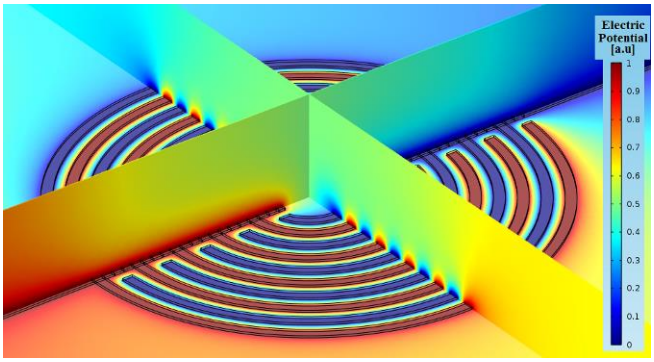

Figure 2. Distribuition of potential field in a 3D RSE structure.

III. NUMERICAL SIMULATION

We have performed different numerical simulations comparing the calculated DC capacitance of IDE, SRE and RSE structures always with the same distance between digits, surface area and same materials and manufacturing process. There are multiple geometrical factors that can be varied in the simulations, but for the sake of clarity, we focus on some of them, keeping fixed the rest. Since the goal is maintaining reduced the surface area of electrodes, we define different widths and distances between digits of the structures given that the lowest safe distance to our manufacturing process is 10µm. Therefore, we have used the number, length and width of fingers and the thickness of the deposited metal film as simulation parameters. Table 1 is a summary of these geometric parameters used for simulation. Remember that fabricated structures for each type of electrode, SRE, IDE and RSE, was made with three distances between digits (10µm, 20µm and 50µm) but the number of electrodes and the thickness of the metal thin film was kept constant.

TABLE I. GEOMETRICAL PARAMETERS OF PLANAR ELECTRODE PAIRS

Parameters	**Electrode type**			***Description***
	RSE	***SRE***	***IDE***	
w	10-50µm	10-50µm	10-50µm	Finger width
g	10-50µm	10-50µm	10-50µm	Gap between fingers
t	2-10µm	2-10µm	2-10µm	Metal film thickness
l	600-800µm	600-800µm	-	Structure length
d	600-800µm	600-800µm	-	Structure width
r	-	-	0.6-3.02mm	Electrode external radium
n	20-50	20-50	20-50	Number of electrodes

 ISBN: 978-1-61208-426-8

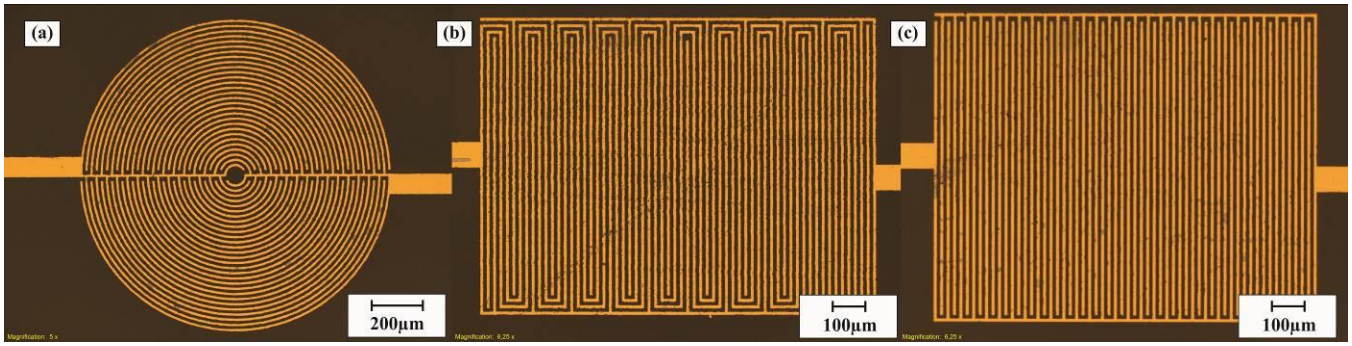

Figure 3. Fabricated RSE (a), SRE (b), and IDE (c) structures.

The first important result was that the capacitance to RSE was the highest in all comparisons. For example, simulating the capacitor with w = 10µm, t = 2µm and 20 electrodes we obtain 2.47pF for RSE while the capacitance for the SRE was 2.45pF and the capacitance for IDE was 2.44pF. This means an increase of capacitance of 30fF between the RSE and the IDE. Whereas electrodes are used as capacitive transducers, the fact of the geometrical factor RSE be higher than in other structures means that the sensitivity of the sensor will always be larger using the same area. Furthermore, the capacitance and the increase in sensitivity will increase proportionally. After that, we calculate the numerical capacitances in order to improve the performance of RSE.

Influence of the width of the electrodes (10 to 50µm) with aspect ratio of the electrode/thickness of the thin film of 5/1 was evaluated for the RSE, SRE and IDE with 20 digits. The results showed a slope of 161.1fF for each micrometer added to the width of the electrodes to the RSE, a slope of 160.7fF/µm for the SRE and 159.3fF/µm for the IDE. Remembering that the surface area of each structure was kept the same for each electrode width.

Electrode length contribution (400 to 800µm) was been evaluated for IDE and SRE electrode with 20 fingers and 10µm of finger width. Results showed the slope of 4.99fF/µm for the SRE and 4.74fF for the IDE.

We also have performed the contribution of finger numbers (n) in each structure. The results are presented in Figure 4, as this contribution is nonlinear.

IV. FABRICATION PROCESS

The electrodes fabrication started with the production of the electrode masks where the IDE, SRE and RSE were designed using high-resolution direct writing photolithography with a laser beam. In the next step, a photoresist layer was deposited onto a square optical glass plate (60mm side Kodak 1A High Resolution Glass) and patterned by conventional ultraviolet light (UV) photolithographic method following the electrodes masks. The UV exposures were carried out in a MJB-3 UV300 contact mask aligner (Karl-Suss, Garching, Germany). Titanium-gold (TiAu) thin films, deposited with a Leybold Univex 300 ebeam evaporator (Cologne, Germany), were used as electrode materials. After thin-film depositions, by the lift-off technic, the devices were immersed in acetone to remove the photoresist layer and excess of metal, leaving the patterned electrodes on the glass surface [6].

V. CHARACTERIZATION

For the experimental characterization the nominal capacitance target was 2pF, taking into account the minimum distance between electrodes of 10µm. Structures with electrode width of 50µm have a total area of 28.26mm², and their dimensions are g = 50µm, l = 5.95mm, d = 4.75mm and r = 3.02mm. The area is 4.52mm² for structures with w = 20µm, g = 20µm, l = 2.38mm, d = 1.90mm and r = 1.21mm. Structures with w = 10µm, minimum secure dimension to our fabrication process, the area is 1.13mm² (g = 10µm, l = 1.19mm, d = 0. 95mm and r = 0.60mm).

The geometric inspection of the fabricated structures was performed using the Olympus BX60 microscope as shown in Figure 3. Electrical characterization has been carried out by measuring their capacitance and parallel resistance using the four-wire measurement with a HP 4284A impedance analyzer (Agilent Tech., Santa Clara, CA, USA). The applied excitation voltage was V_{AC} = 1V and V_{DC} = 0V. The frequency sweep of analysis was from 100Hz to 1MHz. The four-point method was used to minimize the contribution of stray capacitances.

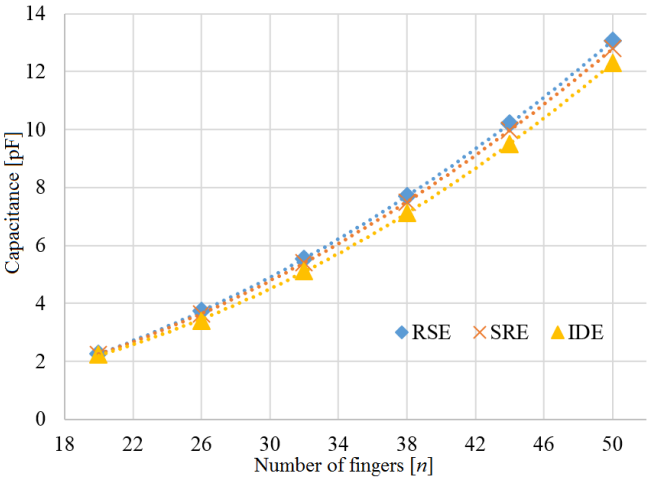

Figura 4. Capacitance vs. number of fingers of RSE, SRE and IDE.

VI. EXPERIMENTAL RESULTS

Measured and the simulated values of the capacitances are in agreement, as shown in Table 2. The measurements were carried out in room conditions (50% RH and 25ºC) at 100 kHz.

TABLE II. NUMERICAL VS. EXPERIMENTAL CAPACITANCE.

Finger width (µm)	**Numerical simulation (pF)**		
	RSE	***SRE***	***IDE***
10	2.4667	2.4446	2.4362
20	4.0906	4.0653	4.0345
50	8.9122	8.8723	8.8091
	Experimental measurement (pF)		
	RSE	***SRE***	***IDE***
10	2.2332	2.2141	2.1917
20	4.2949	4.2667	4.2412
50	10.5385	9.9979	9.7105

Capacitance measured values have a maximum of 12% discrepancy compared to the simulated results. This difference is due to the capacitance of contacts pads that were not included in the simulation and the variability of the fabrication process.

VII. CONCLUSION

A comparison between the capacitances under different geometric parameters of RSE, SRE and the conventional IDE was shown on this work. Numerical simulations of the capacitance have been carried out to calculate the differences between them due exclusively to their geometrical characteristics at constant area. In these conditions, we have shown a slight capacitance increase for the ring-shaped electrodes against the serpentine electrodes and the conventional interdigitated electrodes.

We have validated the numerical results by experimental characterization of ring-shaped, serpentine and interdigitated structures capacitance. Experimental results verified the capacitive differences between the three structures with same area, for 10µm, 20µm and 50µm of finger width. Moreover, ring-shape electrode presents a geometrical morphology that allows the better usage of its area. It is a promising base electrode mainly when used as sensor in application that involves dripping of substances under analysis or dripping of selective/sensitive substances like zeolite.

ACKNOWLEDGMENT

The authors acknowledge the Center for Semiconductor Components (CCS), the Multi-User Laboratory of IFGW (LAMULT), the Device Research Laboratory (LPD) and the Brazilian Synchrotron Light Laboratory (LNLS). Financial support for this project was provided by the National Council for Scientific and Technological Development (CNPq) and the São Paulo State Research Support Foundation (FAPESP) inside the National Institute for Science and Technology of Micro and Nanoelectronic Systems (INCT NAMITEC) project.

REFERENCES

[1] M. I. Rocha-Gaso, C. March-Iborra, Á. Montoya-Baides, and A. Arnau-Vives, "Surface generated acoustic wave biosensors for the detection of pathogens: A review," Sensors, vol. 9, 2009, pp. 5740.

[2] N. A. Ramli and A. N. Nordin, "Design and modeling of MEMS SAW resonator on Lithium Niobate," 4th International Conference On Mechatronics (ICOM), 2011, pp.1-4.

[3] M. W. Kim, Y. H. Song, and J. B. Yoon, "Modeling, fabrication and demonstration of a rib-type cantilever switch with an extended gate electrode," Journal of Micromechanics and Microengineering, vol. 21, 2011, 115009.

[4] R. Mahameed, A. M. El-Tanani, and G. M. Rebeiz, "A zipper RF MEMS tunable capacitor with interdigitated RF and actuation electrodes." Journal of Micromechanics and Microengineering, vol. 20, n. 3, 2010, 035014.

[5] Z. Chen, A. Sepúlveda, M. D. Ediger, and R. Richert, "Dielectric spectroscopy of thin films by dual-channel impedance measurements on differential interdigitated electrode arrays," The European Physical Journal B-Condensed Matter and Complex Systems, vol. 85, n.8, 2012, pp. 1-5.

[6] L. E. B. Ribeiro, M. H. Piazzetta, A. L. Gobbi, J. S. Costa, J. A. F. da Silva, and F. Fruett, "Fabrication and Characterization of an Impedance Micro-Bridge for Lab-on-a-Chip." ECS Transactions, vol. 31, n. 1, 2010, pp. 155-163.

[7] A. Rivadeneyra, J. Fernández-Salmerón, J. Banqueri, J. A. López-Villanueva, L. F. Capitan-Vallvey, and A. J. Palma, "A novel electrode structure compared with interdigitated electrodes as capacitive sensor," Sensors and Actuators B: Chemical, vol. 204, 2014, pp. 552-560.

[8] Y. Kim, B. Jung, H. Lee, H. Kim, K. Lee, and H. Park, "Capacitive humidity sensor design based on anodic aluminum oxide," Sensors and Actuators B: Chemical, vol 141, n. 2, 2009, pp. 441-446.

[9] J. W. Grate and G. C. Frye, "Acoustic wave sensors," Sensors update, vol. 2, 1996, pp. 37-83.

[10] J. Virtanen, L. Ukkonen, T. Bjorninen, and L. Sydanheimo, "Printed humidity sensor for UHF RFID systems," Sensors Applications Symposium (SAS), 2010 IEEE, 2010, pp. 269-272.

[11] D. Briand, A. Oprea, J. Courbat, and N. Bârsan, "Making environmental sensors on plastic foil," Materials Today, vol. 14, n. 9, 2011, pp. 416-423.

[12] R. Igreja and C. J. Dias, "Analytical evaluation of the interdigital electrodes capacitance for a multi-layered structure," Sensors and Actuators A: Physical, vol. 112, n. 2, 2004, pp. 291-301.

[13] M. Urbriztondo, I. Pellejero, A. Rodriguez, M. P. Pina, and J. Santamaria, "Zeolite-coated interdigital capacitors for humidity sensing," Sensors and Actuators B: Chemical, vol. 157, Issue 1, 2011, pp. 450-459.

[14] A. Rivadeneyra, J. Fernández-Salmerón, M. Agudo, J. A. López-Villanueva, L. F. Capitan-Vallvey, and A. J. Palma, "Design and characterization of a low thermal drift capacitive humidity sensor by inkjet-printing," Sensors and Actuators B: Chemical, vol. 195, 2014, pp. 123-131.

 ISBN: 978-1-61208-426-8